



HAL
open science

Degradation Modes estimation tool for Second life Li-ion batteries with inhomogeneous lithium distribution

Lucas Albuquerque, Fabien Lacressonnière, Christophe Forgez, Nicolas Damay, Xavier Roboam

► To cite this version:

Lucas Albuquerque, Fabien Lacressonnière, Christophe Forgez, Nicolas Damay, Xavier Roboam. Degradation Modes estimation tool for Second life Li-ion batteries with inhomogeneous lithium distribution. SYMPOSIUM DE GENIE ELECTRIQUE 2023, L2EP, Jul 2023, Lille, France. hal-04159980

HAL Id: hal-04159980

<https://ut3-toulouseinp.hal.science/hal-04159980>

Submitted on 12 Jul 2023

HAL is a multi-disciplinary open access archive for the deposit and dissemination of scientific research documents, whether they are published or not. The documents may come from teaching and research institutions in France or abroad, or from public or private research centers.

L'archive ouverte pluridisciplinaire **HAL**, est destinée au dépôt et à la diffusion de documents scientifiques de niveau recherche, publiés ou non, émanant des établissements d'enseignement et de recherche français ou étrangers, des laboratoires publics ou privés.

Degradation Modes estimation tool for Second life Li-ion batteries with inhomogeneous lithium distribution

Lucas ALBUQUERQUE¹, Fabien LACRESSONNIÈRE¹, Christophe FORGEZ², Nicolas DAMAY², Xavier ROBOAM¹

¹ LAPLACE, UMR CNRS-INPT-UPS, Université de Toulouse, France ² Roberval, Université de Technologie de Compiègne, France

Abstract – Accurately identifying the sources and rates of degradation in Li-ion batteries is crucial for predicting and mitigating their aging process. A diagnostic tool is presented in this study that can estimate the Degradation Modes (DMs) of Li-ion batteries using the Incremental Capacity Analysis (ICA) technique. To improve the precision of the DMs estimation tool, the software also considers an estimation of the inhomogeneous loss of cyclable lithium within the negative electrode. A range of second life Li-ion batteries with Graphite/NMC622 chemistry was tested in order to evaluate the performance of the diagnostic tool, enabling the comparison of their respective aging characteristics. The results demonstrate that the diagnostic tool provides an effective mean of characterizing and predicting the aging of Li-ion batteries, offering valuable insights into the behavior and performance of these critical energy storage systems.

Keywords – Li-ion, Battery, Degradation Modes, Diagnosis, aging, second life, inhomogeneity, heterogeneity.

1. INTRODUCTION

After a first life in electric vehicles, the battery packs can be dismantled for determining their fitness for second life applications with a remaining State of Health (SoH) of around 80%. The battery module selection procedure is based on several test protocols such as capacity and power measurements. However, the aging mechanisms in the Li-ion battery modules cannot be obtained from these test protocols. Several papers have been published on the estimation of DMs in the literature, but few focused on applying the available techniques in the context of second life [1–12]. Therefore, this paper, which is a follow-up to our last [13], explains the DMs estimation tool developed for second life battery applications.

The diagnostic tool here presented was developed on MATLAB and inspired by many publications, especially the Incremental Capacity Analysis (ICA) method used to quantify the battery DMs published by Matthieu Dubarry et al. [8–10] and on the software developed by Johannes Philipp Fath et al. [11] which can estimate lithium distribution inhomogeneity in Li-ion cells. The goal of this tool is to give an estimation of the DMs taking place inside a Li-ion cell in order to follow the aging process during their second life. This is achieved by obtaining the pseudo Open Circuit Voltage (pOCV) of the battery at different SoHs.

The ICA technique has been extensively used to estimate the SoH of batteries by monitoring the characteristic phase transition peaks during their operation. ICA has been demonstrated to provide accurate evaluations of battery SoH, even under high C-rates, as long as the characteristic peaks are still present in the signature. When estimating DMs, the magnitude of the imposed current is more critical, and lower regimes are linked to more precise results, although some studies have performed high C-rate tests with satisfactory outcomes [14, 15]. ICA appears to be a suitable method for evaluating the overall health of Li-ion battery modules for second-life applications, providing essential information on the remaining useful life and suitability of

a module for a given application. Nonetheless, to streamline the module evaluation process, additional research is necessary to identify the maximum current regimes that can yield practical information when ICA is applied to second-life batteries exhibiting higher impedances.

In this study, three Li-ion batteries of the same technology with a NMC622 cathode and a graphite anode possessing different SoHs were charged and discharged at low currents (C/20) in order to validate the DMs estimation software. This analysis is important to understand how these DMs will impact the battery capabilities to accomplish their missions in second life applications.

2. LI-ION DEGRADATION MODES

There are multiple complex degradation mechanisms taking place in a Li-ion battery during its life [16]. Nonetheless, these mechanisms can be grouped into distinct categories based on their overall macroscopic impact (see Fig. 1). The effects modeled by the diagnostic tool are:

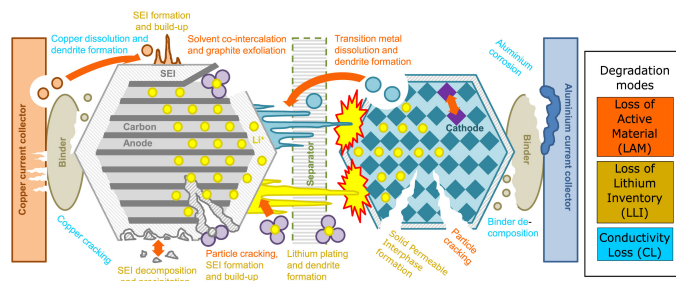


Figure 1. Degradation mechanisms in a Li-ion battery (Original figure from [16] and modified in [17]).

The first one is the Loss of Lithium Inventory (LLI), which is the main cause of aging during the battery first cycles. Lithium ions are mainly consumed due to the side reactions that form the Solid Electrolyte Interphase (SEI) layer on the graphite anode. The SEI is a naturally formed passivation layer which protects the anode from the electrolyte, but it is further thickened during battery usage where the lithium ions react with the compounds found in the electrolyte to form said layer. The electrolyte composition is of crucial importance to the stability of this layer, commonly being constituted of Ethylene carbonate (EC), Dimethyl carbonate (DMC), Diethyl carbonate (DEC) and additives such as Vinylene carbonate (VC). It has been proved that for nickel rich NMC cathodes, a small part of LLI can be attributed to the Cathode Electrolyte Interphase (CEI). Another effect that causes LLI is the lithium plating mechanism. This phenomenon occurs when the anode potential drops below 0 V (during high charging rates and low temperatures) and metallic lithium is deposited on the electrode surface.

The second and third DMs are the Loss of Active Material

of the negative and positive electrodes (LAM_{NE} and LAM_{PE}), which are consequences of the volume expansion and contraction suffered by the electrodes during cycling. Whenever these DMs occur, the possible sites for lithium ion insertion get disconnected from the main active particle and no longer interact with the conducting matrix. These isolated particles can get disconnected with the presence (or not) of lithium inside the active material, so this particular DM would be accompanied by LLI. Other reasons such as transition metal dissolution or graphite exfoliation can also be the cause of these DMs. Particularly for NMC batteries, Manganese dissolution has been reported and is known to migrate to the SEI and contaminate this layer, intensifying battery aging by promoting further electrolyte decomposition [18].

The last effect worth mentioning is the inhomogeneous Li^+ distribution, which is not a DM on itself, but rather a consequence of aging in large electrode active surfaces [11]. This phenomenon is more noticeable with more aged cells and could possibly be attributed to a spatial variation of Li^+ concentration on the electrode, causing a local State of Charge (SoC) dispersion in the cell. Towards lower SoHs, the cells can present lithium plating on some regions of the anode.

3. THE DEGRADATION MODES ESTIMATION TOOL

As previously mentioned, this DMs estimation tool will be used to further understand the aging mechanisms taking place in the second life Li-ion batteries. In order to identify the initial cell parameters and afterward the DMs, the tool relies on a simple optimization algorithm that generates multiple Incremental Capacity (IC) curves from the half-cell pOCVs and selects the one which minimizes the cumulative Root-Mean-Square Error (RMSE) between the simulated and experimental curves for each voltage value. These simulated pOCV curves are created by changing the electrodes Loading Ratios (LR), which is the capacity proportion between both active materials, and the Offset between the negative and positive electrode curves. With this (LR, Offset) pair, the half-cell pOCV curves and the experimental capacity of the battery, it is possible to recreate a simulated pOCV curve. Fig. 2 shows a schematic view of the functions to be described in the following paragraphs.

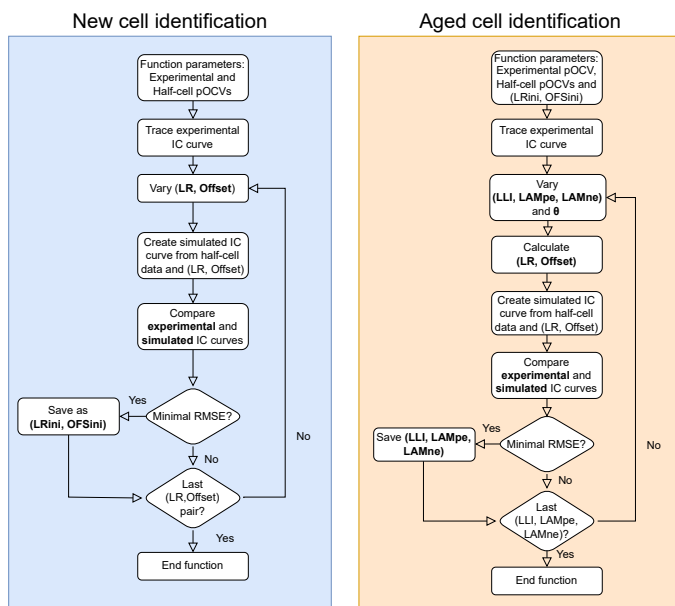


Figure 2. Identification functions of the DMs estimation tool.

3.1. New cell identification

The first identification function is the reference for the following DMs estimations, it receives the experimental pOCV curve of a given battery as input and calculates the associated experimental IC curve. In order to calculate the simulated IC curves, a first step of adjusting both half-cell pOCVs is necessary. First the negative electrode pOCV ($pOCV^-$) is shifted by the Offset and then scaled with the LR value (as seen in Fig. 3). The positive electrode pOCV ($pOCV^+$) remains unaltered, since this last is used as the reference for the full cell SoC. Then, if the Offset value is positive, the $pOCV^+$ is subjected to interpolation with the negative electrode SoC values in order to add both curves and create the simulated full-cell. Fig. 3 illustrates this step. Subsequently the simulated IC curve for the given (LR, Offset) pair is calculated.

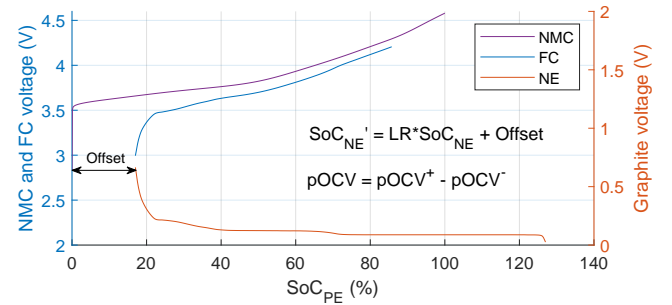


Figure 3. Full cell determination procedure from half-cells pOCVs.

This process is repeated for each (LR, Offset) pair and compared with the experimental IC curve. The result with the smallest cumulative RMSE is retained as the reference cell at 100% SoH for the following function. The following equation is used to calculate the RMSE between the experimental and simulated IC curves. Here, N is the number of points in the window containing the IC peaks, set to 3.2 V and 4.15 V.

$$RMSE = \sqrt{\frac{1}{N} \sum_{j=1}^N (IC_{Experimental}(j) - IC_{simulated}(j))^2} \quad (1)$$

3.2. Aged cell identification

The second identification function, as in the first, receives the experimental pOCV curve to calculate its IC signature. It then creates the simulated IC curves by trying multiple combinations of the triplet (LLI, LAM_{PE} , LAM_{NE}) that will ultimately modify the original values of (LR, Offset) according to the following equations (modified from [8]).

$$LR = LR_{ini} \frac{100\% - \%LAM_{NE}}{100\% - \%LAM_{PE}} \quad (2)$$

$$Offset = Offset_{ini} + \%LLI - \frac{LR}{LR_{ini}} \%LAM_{PE} \quad (3)$$

Here, $(LR_{ini}, Offset_{ini})$ are the initial parameters found for the cell with 100% SoH. The following step is taking into account the inhomogeneous lithium distribution. It is known that as the cell ages, the negative electrode can present a spatial dispersion of lithium distribution across its surface [23]. This phenomenon could possibly be attributed to an heterogeneous current density across the electrode, inducing local hot spots in the cell and thus LLI (with possible lithium plating). This degradation effect is modeled by a third and last function of the DM

estimation tool. Its inputs are the (LR, Offset) pair of the aged cell, which is the result of the previous function, as well as its POCV curve. The procedure is possible thanks to the superposition property of the IC curve, for which the sum of multiple parallel cell voltages is the response of the battery. This is done by dividing the original cell into multiple virtual parts (11 in this work) and simulating a LLI gradient around the Offset value of the real cell, since LLI is directly translated into a shift of the negative electrode. Each virtual cell will have a different percentage of Li^+ loss, but the average of all the virtual parts is the same as the real cell. The following equation, modified from the article by J.P Fath et al. [11], equates this phenomenon:

$$Offset = Offset_{mean} + \left(\frac{cell}{10} - 5\right) * \theta \quad (4)$$

In which ($cell \in \mathbf{N} | cell \in [0, 10]$) is the virtual cell number and θ is the total LLI gradient range in percent. In practice, a large θ means that the cell presents a high lithium distribution heterogeneity and each virtual cell used to create the experimental signature has a different LLI value. Here, as in [11], a linear LLI distribution has been chosen to model the dispersion. Note that since the input of this function is the output of the previous, any inaccuracies found in the former in terms of DMs are propagated to the latter. This was prevented by inserting the inhomogeneous lithium distribution function inside the DMs estimation function. However, this means that for any triplet (LLI, LAM_{PE} , LAM_{NE}) tested, the inhomogeneous lithium distribution test has to be done in sequence, making the simulation computationally heavier, although still feasible. The triplet and θ capable of minimising the RSME are stored.

The choice of whether implementing the inhomogeneous lithium distribution function inside the main identification loop or after it depends mainly on the SoH of the cell to be identified. For less aged cells, since they present well defined IC peaks, the overall identified IC shape without inhomogeneities taken into account can represent accurately the experimental one. Therefore, in such cases, the inhomogeneity function can be placed outside the loop to simplify the process. However, for cells with higher degrees of aging and thus flatter IC signatures, the inclusion of the inhomogeneity step within the primary function loop becomes essential. This is due to the fact that for such cells, no triplet (LLI, LAM_{PE} , LAM_{NE}) would be able to accurately model its flatter IC shape, propagating the inaccurate result to the inhomogeneity loop. This last remark is developed in the next section.

4. APPLICATION

In order to validate the DMs estimation tool, three Li-ion NMC622/Graphite cells issued from hybrid electric vehicles used packs were extracted. Since they come from different packs, their first lives were not exactly the same. For each cell, the IC curve was plotted from a measurement of the cell voltage during a charge protocol with low current (C/20) between 2.7 V and 4.2 V at ambient temperature (23°C). Fig. 4 displays the three experimental IC curves of the aforementioned cells. The cell with 100% SoH presents well defined phase transition peaks as expected for a new battery. The cell with 86.2% SoH also exhibits well pronounced peaks, however with lower amplitudes when compared with the pristine cell. Finally, the 82.8% SoH cell shows the most flawed signature, as this last has lost the last distinct graphite phase transition peak, while the remaining peaks appear broader and smaller in amplitude.

It is already known that for cells with higher aging, their IC curves present lower peak amplitudes due to LLI and LAM [8]. This trend is confirmed when comparing the three experimental curves at different SoHs (Fig. 4). As explained in section 3, the cell with 100% SoH, set as the reference for the others, was the first to be subjected to the tool. Its parameters were then used as inputs for the following functions, together with the remaining two batteries POCV curves. Ideally, the tool should be applied

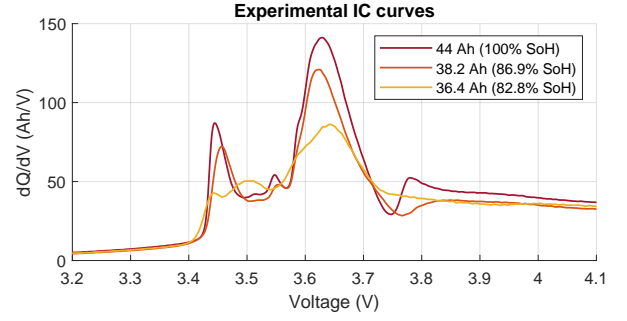


Figure 4. Experimental IC plots for the three cells at different SoHs.

to the same battery at multiple SoHs, in order to track the DMs throughout its lifetime. Fig. 5 shows the experimental IC curves of each battery as well as the identified curves with and without Li^+ inhomogeneity taken into account.

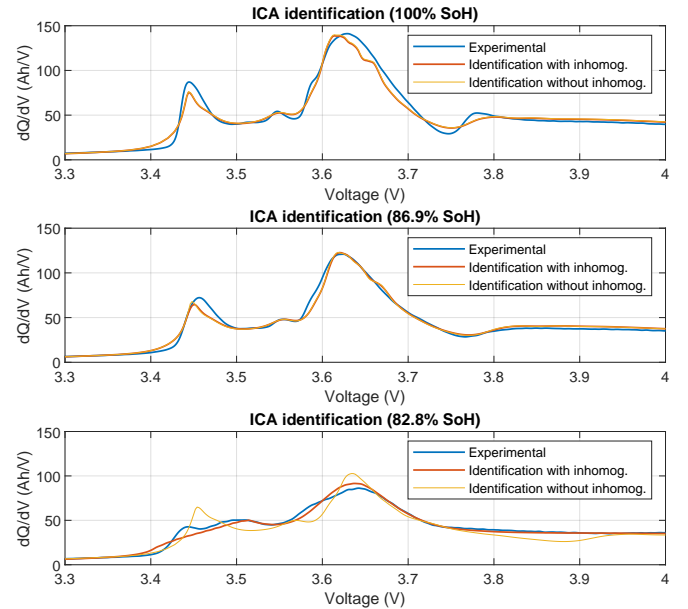


Figure 5. Simulated IC plots for the three cells at different SoH.

The identification results shown in Fig. 5 are satisfactory, as the overall shapes of the IC curves are captured by the estimation tool with minor local errors (see Tab. 1). The initial two cells tested exhibited minimal levels of Li^+ inhomogeneity, which was anticipated given their well-defined shapes. On the other hand, as seen on Fig. 4, the most aged cell presents a much flatter IC signature when compared to the cell with 86.9% SoH, despite the fact that their capacity difference is not substantial. This could be explained by a higher Li^+ inhomogeneity for the more degraded cell. In the last plot from Fig. 5, it is clear that the experimental IC peaks more closely resemble the identification function with inhomogeneity taken into account (in the inner identification loop), as this last tends to widen peaks and reduce their amplitudes. The observed effect can be attributed to the simultaneous phase transitions occurring at slightly different voltages in distinct regions of the anode [22, 23].

Fig. 6 shows the DMs obtained with the estimation tool and the θ value for the three cells. Note that LLI and LAM_{PE} are the main aging mechanisms associated with capacity fade, this is a known trend for NMC batteries [23, 24]. They mainly contribute to the loss in amplitude of the IC peak situated between 3.6 V

Table 1. Minimal RMSE between the experimental and simulated IC curves.

RMSE (Experimental - simulated) [Ah/V]	100% SoH	86.9% SoH	82.8% SoH
With inhomogeneity	4.47	3.06	2.35
Without inhomogeneity	4.47	3.11	5.74

and 3.7 V. As for the first identified peak between 3.4 V and 3.5 V directly associated to the first phase transitions in the graphite electrode, its flattened out signature is linked to the Li^+ inhomogeneity increase, since no LAM_{NE} has been identified for the most aged cell. The high inhomogeneity value identified can be explained by a probable amount of lithium plating consuming Li^+ in addition to the SEI layer, for the cell with 82.8% SoH. Whereas the LLI for the 86.9% SoH cell is only due to the passivation layer, since the Li^+ inhomogeneity value is much lower for this last. It is crucial to acknowledge that this assertion is solely based on the high inhomogeneity value obtained through the tool. The veracity of this supposition can only be proved by conducting a post-mortem analysis of the electrode surfaces or through an in-depth investigation of the SEI and charge transfer resistances utilizing, for example, a pulse characterization method to precisely quantify the individual contributions to the overall surface resistance [19–21].

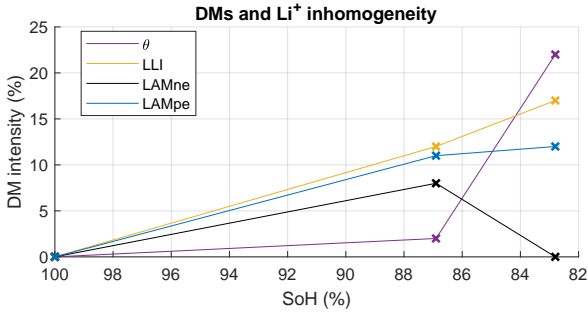


Figure 6. Degradation Modes in function of capacity loss.

In order to better understand the DM results obtained with the tool, Fig. 7 portrays the Differential Voltage (DV) plot for the three cells. Since the peaks of this plot highlight not the phase transitions, but the existence of just one phase in the graphite electrode, a direct inter-peak measurement can give the extent of LAM_{NE} [12]. This procedure yielded a LAM_{NE} of 10.15% for the cell with 86.9% SoH, which is close the 8% given by the estimation tool. As for the most aged cell, this technique is not applicable, since no visible peak is recognised before the last graphite phase transition towards higher capacities. Nonetheless, a plateau-like form is present and helps to visualise the extent of the Li^+ inhomogeneity identified with the tool.

The robustness of our results given by the DMs estimation tool was verified, nevertheless, in order to enhance its reliability and accuracy, further improvements to the tool are necessary and will be pursued. Additional aging data will be incorporated to refine and enhance the tool's performance in the future. As seen in Fig. 6, LAM_{NE} is null for the cell with higher capacity loss. Although possible, this value is rather unlikely for a cell aged to this extent. This might be due to a difficulty of the algorithm in distinguishing the more flatter IC signature of this last cell. Distinguishing LAMs with and without lithium trapped inside the electrodes could probably help to get more precise results. However, in [11], which examined the same battery technology as in this study, it was observed that for the majority of the ag-

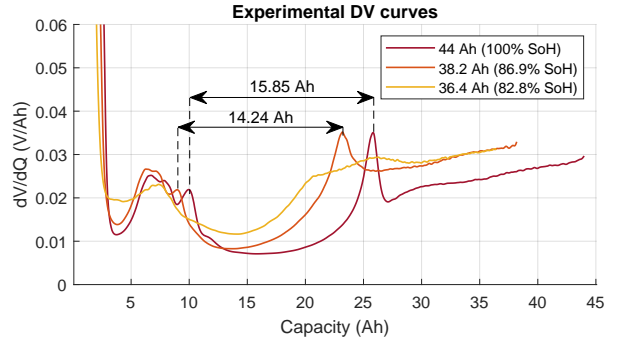


Figure 7. Experimental Differential Voltage for the three analysed cells.

ing profiles, either no LAM_{NE} was verified or a net increase in the total negative electrode capacity was observed. This corroborates to the possibility of having no or negligible LAM_{NE} for the most aged battery.

As for the Li^+ inhomogeneity estimation, a possible point for improvement is the distribution function itself. In [22], the possibility of having different Offset dispersions is mentioned. This would help to explain why in Fig. 4, for the most aged cell, two distinct peaks appear between 3.4 V and 3.55 V. In this case specifically, maybe two distinct Offset gradients superposed could better capture the Li^+ inhomogeneity distribution.

Moreover, a crucial consideration for the effective utilization of this type of tool is the half-cell data employed. It is a well-established fact that the half-cell pOCVs deteriorate as they age [25], and incorporating diverse half-cell data could enhance the identification of older cell signatures. Furthermore, the electrodes exhibit rate dependence, and as LAM progresses, their effective active surface area diminishes, resulting in the accentuation of kinetic effects. In this study, this issue was circumvented by imposing low currents. However, in order to apply the tool on a large scale, the development of a rate-dependent algorithm is of utmost importance for faster and more accurate testing, specially for the selection of second life batteries.

Moving forward, this diagnostic tool will be utilized to study second life battery modules until the end of their useful life, providing valuable insights into their performance and behavior over time. By utilizing the information derived from this tool, it becomes feasible to forecast the battery aging knee [26] and generate accurate prognostic assessments of the system's overall health. This diagnosis at the beginning of a battery's second life is vital for the development of second life battery energy systems and for mitigating the ecological impact of these elements.

5. CONCLUSIONS

The identification of aging mechanisms in second life Li-ion batteries is crucial for the development of effective battery management strategies that can prolong their useful lifespan. The presented DMs identification tool has exhibited promising results in accurately estimating the primary sources of aging in such batteries. Notably, while this type of methodology is typically employed for first life batteries, its applicability to second life batteries represents a significant step towards the optimal utilization of these resources. The accurate identification of aging mechanisms in second life Li-ion batteries is critical for ensuring their safety and reliability, as well as for mitigating the environmental impact of battery disposal. The DMs identification tool, with its capability of pinpointing the root causes of aging in these batteries, holds immense potential in advancing the development of sustainable and efficient energy storage solutions.

In addition, the ongoing second life battery aging campaign presents a unique opportunity to further refine and enhance the performance of the DMs identification tool. By utilizing addi-

tional aging data, the tool's accuracy and reliability can be further improved, leading to even more precise and effective battery management strategies.

6. ACKNOWLEDGEMENTS

This work has been supported by the OCCITANIE Region in the framework of the B2LIVE project.

7. REFERENCES

- [1] A. Barai et al., "A comparison of methodologies for the non-invasive characterisation of commercial Li-ion cells", *Progress in Energy and Combustion Science*, Volume 72, 2019, Pages 1-31, ISSN 0360-1285, <https://doi.org/10.1016/j.pecs.2019.01.001>.
- [2] C. Pastor-Fernández et al., "A SoH diagnosis and prognosis method to identify and quantify degradation modes in Li-ion batteries using the IC/DV technique", 6th Hybrid and Electric Vehicles Conference (HEVC 2016), London, UK, 2016, pp. 1-6, doi: 10.1049/cp.2016.0966.
- [3] T. Plattard, S. Franger et al., "Combining a Fatigue Model and an Incremental Capacity Analysis on a Commercial NMC/Graphite Cell under Constant Current Cycling with and without Calendar Aging". *Batteries* 2019, 5, 36. <https://doi.org/10.3390/batteries5010036>.
- [4] C. Pastor-Fernández et al., "A Comparison between Electrochemical Impedance Spectroscopy and Incremental Capacity-Differential Voltage as Li-ion Diagnostic Techniques to Identify and Quantify the Effects of Degradation Modes within Battery Management Systems", *Journal of Power Sources*, Volume 360, 2017, Pages 301-318, ISSN 0378-7753, <https://doi.org/10.1016/j.jpowsour.2017.03.042>.
- [5] T. Raj et al., "Investigation of Path-Dependent Degradation in Lithium-Ion Batteries", *Batteries & Supercaps*, vol. 3, number 12, pages 1377-1385, <https://doi.org/10.1002/batt.202000160>.
- [6] J. Chen et al., "Peak-tracking method to quantify degradation modes in lithium-ion batteries via differential voltage and incremental capacity", *Journal of Energy Storage*, Volume 45, 2022, 103669, ISSN 2352-152X, <https://doi.org/10.1016/j.est.2021.103669>.
- [7] Hannah M. Dahn et al., "User-Friendly Differential Voltage Analysis Free-ware for the Analysis of Degradation Mechanisms in Li-Ion Batteries", 2012, *J. Electrochem. Society*, 159, A1405.
- [8] M. Dubarry et al., "Synthesize battery degradation modes via a diagnostic and prognostic model", *Journal of Power Sources*, vol. 219, p. 204-216, 2012.
- [9] M. Dubarry et al., "Cell degradation in commercial LiFePO4 cells with high-power and high-energy designs", *Journal of Power Sources*, vol. 258, 2014, Pages 408-419, ISSN 0378-7753, <https://doi.org/10.1016/j.jpowsour.2014.02.052>.
- [10] M. Dubarry and D. Beck, "Perspective on Mechanistic Modeling of Li-Ion Batteries", *Accounts of Materials Research*, vol. 3, number 8, pages 843-853, 2022, 10.1021/accountsmr.2c00082.
- [11] J.P. Fath et al., "Quantification of aging mechanisms and inhomogeneity in cycled lithium-ion cells by differential voltage analysis", *Journal of Energy Storage*, vol. 25, p. 100813, 2019.
- [12] M. Lewerenz et al., "Differential voltage analysis as a tool for analyzing inhomogeneous aging: A case study for LiFePO4/Graphite cylindrical cells", *Journal of Power Sources*, Volume 368, 2017, Pages 57-67, ISSN 0378-7753, <https://doi.org/10.1016/j.jpowsour.2017.09.059>.
- [13] L. Albuquerque et al., "Incremental Capacity Analysis as a diagnostic method applied to second life Li-ion batteries", *Electrimacs 2022 Conference*, Nancy, France, 2022.
- [14] J. Choi et al., "Rapid determination of lithium-ion battery degradation: High C-rate LAM and calculated limiting LLI", *Journal of Energy Chemistry*, Volume 67, 2022, Pages 663-671, ISSN 2095-4956, <https://doi.org/10.1016/j.jechem.2021.11.009>.
- [15] M. Maures et al., "Impact of temperature on calendar ageing of Lithium-ion battery using incremental capacity analysis", *Microelectronics Reliability*, Volumes 100-101, 2019, 113364, ISSN 0026-2714, <https://doi.org/10.1016/j.microrel.2019.06.056>.
- [16] Christoph R. Birkl et al., "Degradation diagnostics for lithium ion cells", *Journal of Power Sources*, Volume 341, 2017, Pages 373-386, ISSN 0378-7753, <https://doi.org/10.1016/j.jpowsour.2016.12.011>.
- [17] C. Pastor-Fernández et al., "Critical review of non-invasive diagnosis techniques for quantification of degradation modes in lithium-ion batteries", *Renewable and Sustainable Energy Reviews*, Volume 109, 2019, Pages 138-159, ISSN 1364-0321, <https://doi.org/10.1016/j.rser.2019.03.060>.
- [18] A. Smith et al., "Investigating the dominant decomposition mechanisms in lithium-ion battery cells responsible for capacity loss in different stages of electrochemical aging", *Journal of Power Sources*, vol. 543, 2022, 231842, ISSN 0378-7753, <https://doi.org/10.1016/j.jpowsour.2022.231842>.
- [19] N. Damay et al., "Separation of the charge transfers and solid electrolyte interphase contributions to a battery voltage by modeling their non-linearities regarding current and temperature", *Journal of Power Sources*, vol. 516, 2021, 230617, ISSN 0378-7753, <https://doi.org/10.1016/j.jpowsour.2021.230617>.
- [20] F. Vendrame et al., "Influence of aging on SEI and charge transfer resistances and their dependence on current and temperature for a Li-ion NCA+NMC/graphite cell", *Electrimacs 2022 Conference*, Nancy, France, 2022.
- [21] H. Rabab et al., "Modeling the non-linearities of charge-transfers and solid electrolyte interphase resistances for a sodium-ion battery with a hard carbon electrode", *Electrimacs 2022 Conference*, Nancy, France, 2022.
- [22] M. Lewerenz et al., "Evaluation of cyclic aging tests of prismatic automotive LiNiMnCoO2-Graphite cells considering influence of homogeneity and anode overhang", *Journal of Energy Storage*, vol. 18, 2018, Pages 421-434, ISSN 2352-152X, <https://doi.org/10.1016/j.est.2018.06.003>.
- [23] J. Sieg et al., "Local degradation and differential voltage analysis of aged lithium-ion pouch cells", *Journal of Energy Storage*, vol. 30, 2020, 101582, ISSN 2352-152X, <https://doi.org/10.1016/j.est.2020.101582>.
- [24] M. Bercebar et al., "Degradation Mechanism Detection for NMC Batteries based on Incremental Capacity Curves", *World Electr. Veh. J.* 2016, 8, 350-361. <https://doi.org/10.3390/wevj8020350>.
- [25] Hyung-Joo Noh et al., "Sungjune Youn, Chong Seung Yoon, Yang-Kook Sun, Comparison of the structural and electrochemical properties of layered Li[NixCoyMnz]O2 (x = 1/3, 0.5, 0.6, 0.7, 0.8 and 0.85) cathode material for lithium-ion batteries", *Journal of Power Sources*, Volume 233, 2013, Pages 121-130, ISSN 0378-7753, <https://doi.org/10.1016/j.jpowsour.2013.01.063>.
- [26] Peter M. Attia et al., "Review—"Knees" in Lithium-Ion Battery Aging Trajectories", 2022, *J. Electrochem. Society*, 169, 060517.